Prediction of Orbital Ordering in Single-Layered Ruthenates

Takashi Hotta[1] and Elbio Dagotto[2]

[1]*Advanced Science Research Center, Japan Atomic Energy Research Institute, Tokai, Ibaraki 319-1195, Japan*
[2]*National High Magnetic Field Laboratory, Florida State University, Tallahassee, Florida 32306*

The key role of the orbital degree of freedom to understanding the magnetic properties of layered ruthenates is discussed based on the 3-orbital Hubbard model coupled to lattice distortions, using numerical and mean-field techniques. In the G-type antiferromagnetic phase of Ca_2RuO_4, recent x-ray experiments reported 0.5 holes/site in the d_{xy} orbital, while d_{yz} and d_{zx} orbitals contain 1.5 holes. This unexpected t_{2g} hole distribution is explained by a novel orbital ordered (OO) state, stabilized by a combination of Coulombic and lattice effects. The phase diagram suggests the possibility of large magnetoresistance effects and a new ferromagnetic OO phase in ruthenates.

The single-layered ruthenate Sr_2RuO_4 has recently attracted much attention, both in its experimental and theoretical aspects, since it is an exotic material exhibiting triplet superconductivity in the solid state [1]. By analogy with superfluidity in ^{3}He, the triplet superconductivity is believed to originate from ferromagnetic (FM) spin fluctuations enhanced by the Hund coupling [2]. In addition to the triplet superconductivity, ruthenates exhibit complex magnetic properties. When Sr is partially substituted by Ca, superconductivity is rapidly destroyed and a paramagnetic metallic phase appears, while for $Ca_{1.5}Sr_{0.5}RuO_4$, a nearly FM metallic phase has been suggested. Upon further substitution, the system eventually transforms into an antiferromagnetic (AFM) insulator [3]. The G-type AFM phase in Ca_2RuO_4 is characterized as a standard Néel state with spin $S = 1$ [4].

In $Ca_{2-x}Sr_xRuO_4$, the Ru^{4+} ion contains four electrons in the $4d$ orbitals. Since the crystal field splitting between e_g and t_{2g} orbitals is larger than the Hund coupling, the Ru^{4+} ion is in the low-spin state ($S = 1$): three up and one down (or three down and one up) electrons occupy the triply degenerate t_{2g} manifold, spanned by d_{xy}, d_{yz}, and d_{zx}. To understand the Néel state of Ca_2RuO_4 observed in experiments, one may consider the tetragonal crystal field effect, leading to the splitting between xy and $\{yz, zx\}$ orbitals, where the xy-orbital state is lower in energy than the other levels. When the xy orbital is fully occupied, a simple superexchange interaction at strong Hund coupling can stabilize the AFM state.

However, recent x-ray absorption spectroscopy studies have revealed that $n_{xy}:n_{yz} + n_{zx} = 1/2:3/2$ (n_γ is the hole number per site at the γ orbital) [5], indicating that the above naive picture based on crystal field effects is incomplete. In addition, a substantial orbital angular momentum has been detected [5], suggesting the existence of spin-orbit coupling in ruthenates. These experimental facts denote that the orbital degree of freedom plays a more crucial role in the magnetic ordering in ruthenates than previously anticipated. Moreover, the importance of magnetoelastic coupling has been experimentally pointed out

in ruthenates [6]. Thus, these oxides belong to the family of "spin-orbital-lattice" complex systems, which are quite difficult to study theoretically.

In this Letter, as a first step toward the solution of this complicated problem, the 3-orbital Hubbard model tightly coupled to lattice distortions is analyzed using numerical and mean-field techniques. Spin-orbit coupling will be incorporated in a future publication. An important conclusion of our analysis is that the G-type AFM phase is stabilized only when *both* Coulombic and phononic interactions are taken into account. The existence of a novel orbital ordering is crucial to reproduce the peculiar hole arrangement observed in experiments [5]. Another interesting consequence of our paper is the possibility of large magnetoresistance phenomena in ruthenates, since in our phase diagram the "metallic" FM phase is adjacent to the "insulating" AFM state. This two-phase competition is at the heart of colossal magnetoresistance (CMR) in manganites [7], and, thus, a CMR-like phenomenon could also exist in ruthenates.

As mentioned above, four electrons exist in t_{2g} orbitals, but these electrons can move to the neighboring Ru sites via the oxygen $2p\pi$ orbitals. In addition, they are correlated with each other and are coupled to the distortion of the RuO_6 octahedron. This situation is described by the Hamiltonian $H = H_{kin} + H_{el-el} + H_{el-ph}$. The first term H_{kin} denotes the hopping of t_{2g} electrons, given by

$$H_{kin} = - \sum_{\mathbf{i}\mathbf{a}\gamma\gamma'\sigma} t^{\mathbf{a}}_{\gamma\gamma'} d^{\dagger}_{\mathbf{i}\gamma\sigma} d_{\mathbf{i}+\mathbf{a}\gamma'\sigma}, \qquad (1)$$

where $d_{\mathbf{i}\gamma\sigma}$ is the annihilation operator for a t_{2g} electron with spin σ in the γ orbital at site $\mathbf{i}$ ($\gamma = xy$, yz, and zx), $\mathbf{a}$ is the vector connecting nearest-neighbor sites, and $t^{\mathbf{a}}_{\gamma\gamma'}$ is the nearest-neighbor hopping amplitude between γ and γ' orbitals along the $\mathbf{a}$ direction via the oxygen $2p\pi$ bond, given by $t^{\mathbf{x}}_{xy,xy} = t^{\mathbf{x}}_{zx,zx} = t^{\mathbf{y}}_{xy,xy} = t^{\mathbf{y}}_{yz,yz} = t = 1$, and zero otherwise. Note that only the two-dimensional case is considered throughout this paper.

The second term H_{el-el} denotes the Coulomb interactions between t_{2g} electrons, given by

$$H_{el-el} = U \sum_{\mathbf{i},\gamma} \rho_{\mathbf{i}\gamma\uparrow}\rho_{\mathbf{i}\gamma\downarrow} + U'/2 \sum_{\mathbf{i}\gamma\neq\gamma'} \rho_{\mathbf{i}\gamma}\rho_{\mathbf{i}\gamma'}$$
$$+ J/2 \sum_{\mathbf{i},\sigma,\sigma',\gamma\neq\gamma'} d^\dagger_{\mathbf{i}\gamma\sigma}d^\dagger_{\mathbf{i}\gamma'\sigma'}d_{\mathbf{i}\gamma\sigma'}d_{\mathbf{i}\gamma'\sigma}$$
$$+ J'/2 \sum_{\mathbf{i},\sigma\neq\sigma',\gamma\neq\gamma'} d^\dagger_{\mathbf{i}\gamma\sigma}d^\dagger_{\mathbf{i}\gamma\sigma'}d_{\mathbf{i}\gamma'\sigma'}d_{\mathbf{i}\gamma'\sigma}, \quad (2)$$

where $\rho_{\mathbf{i}\gamma\sigma} = d^\dagger_{\mathbf{i}\gamma\sigma}d_{\mathbf{i}\gamma\sigma}$, $\rho_{\mathbf{i}\gamma} = \sum_\sigma \rho_{\mathbf{i}\gamma\sigma}$, U (U') is the intra- (inter)orbital Coulomb interaction, J is the inter-orbital exchange interaction, and J' is the pair-hopping amplitude between different orbitals. Note that $U = U' + J + J'$ due to rotational invariance in orbital space and $J' = J$ from the evaluation of Coulomb integrals.

Finally, the third term H_{el-ph} indicates the electron-lattice coupling, expressed as [8]

$$H_{el-ph} = g \sum_{\mathbf{i}} (Q_{z\mathbf{i}}\rho_{\mathbf{i}xy} + Q_{x\mathbf{i}}\rho_{\mathbf{i}yz} + Q_{y\mathbf{i}}\rho_{\mathbf{i}zx})$$
$$+ (k/2) \sum_{\mathbf{i}} (Q^2_{2\mathbf{i}} + Q^2_{3\mathbf{i}}), \quad (3)$$

where g is the electron-lattice coupling constant, $Q_{x\mathbf{i}} = (-1/2)Q_{3\mathbf{i}} + (\sqrt{3}/2)Q_{2\mathbf{i}}$, $Q_{y\mathbf{i}} = (-1/2)Q_{3\mathbf{i}} - (\sqrt{3}/2)Q_{2\mathbf{i}}$, $Q_{z\mathbf{i}} = Q_{3\mathbf{i}}$, and k is the spring constant. Here $Q_{2\mathbf{i}}$ and $Q_{3\mathbf{i}}$ are the $(x^2 - y^2)$- and $(3z^2 - r^2)$-mode distortions of the RuO_6 octahedron, respectively. The self-trapping energy is defined as $E_{ph} = g^2/(2k)$. Since oxygens are shared by adjacent octahedra, the distortions do not occur independently, and a cooperative treatment should be employed in this problem. A simple way to include such an effect is to optimize directly the displacement of oxygen ions [7]. In practice, considering sites $\mathbf{i}$ and $\mathbf{i} + \mathbf{a}$, the oxygen in between is allowed to move only *along* the $\mathbf{a}$ axis (neglecting buckling and rotations), while apical oxygens move freely along the z direction.

This model is believed to provide a good starting point to study the electronic properties of ruthenates, but it is difficult to solve even approximately. To gain insight into this complex system, an unbiased technique should be employed. Thus, in this paper, first a small 2×2 plaquette cluster is analyzed [9] by using the Lanczos algorithm to determine the exact diagonalization [10] and the relaxation technique to determine the oxygen positions [11].

The main result of this paper is summarized in the ground state phase diagram shown in Fig. 1(a) for $J = 3U'/4$ [12]. There are six phases in total, which are divided into two groups. One group is composed of phases stemming from the $U' = 0$ or $E_{ph} = 0$ limits. The origin of these phases will be addressed later, but first their main characteristics are briefly discussed. For $E_{ph} = 0$, a C-type AFM orbital disordered (OD) phase appears in the region of small and intermediate U'. This state is characterized by $n_{xy}:n_{yz} + n_{zx} = 1/2:3/2$. Hereafter, a short-hand notation such as "1/2:3/2" is used to denote the hole configuration. For large U', and still $E_{ph} = 0$, a FM/OD
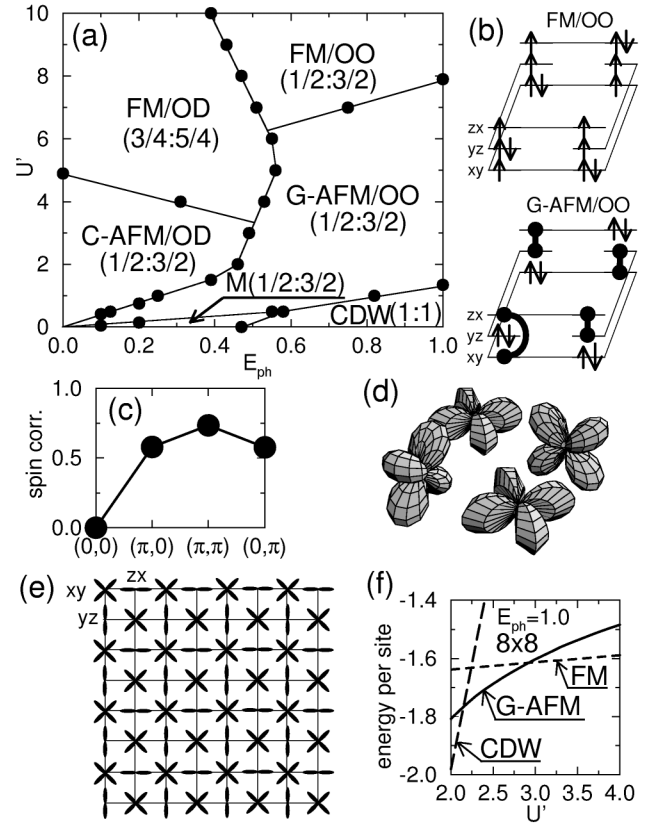

FIG. 1. (a) Ground state phase diagram for the full model with $J = 3U'/4$. The notation is explained in the text. (b) Electron configurations in t_{2g} orbitals for the FM/OO and G-AFM/OO states. Solid circles connected by solid curves denote the local $S = 1$ spin. Thin lines connecting orbitals denote the allowed hopping processes. (c) Spin correlation for the G-AFM phase. (d) Orbital pattern for FM/OO and G-AFM/OO states. (e) Orbital ordering in ruthenates, deduced from the 2×2 result. (f) Mean-field energies for CDW, G-AFM, and FM states on the 8×8 lattice and $E_{ph} = 1.0$, with lattice distortions assumed from the exact 2×2 results.

phase characterized by 3/4:5/4 is stable, which may correspond to Sr_2RuO_4. On the other hand, for $U' = 0$ and small E_{ph}, a metallic (M) phase with small lattice distortion is observed, while for large E_{ph}, a charge-density-wave (CDW) state characterized by 1:1 was found. In short, the G-type AFM phase observed experimentally [4] does *not* appear for $E_{ph} = 0$ or for $U' = 0$.

Another group includes two phases which are not connected to either $E_{ph} = 0$ or $U' = 0$. It is only in this group, with *both* lattice and Coulomb effects being relevant, that for intermediate U' the G-type AFM and the orbital ordered (OO) phase with 1/2:3/2 found in experiments [5] is stabilized. At larger U', a FM/OO phase occurs with the same hole arrangement. The electron configurations for the FM and AFM phases are summarized in Fig. 1(b). In the FM phase, since an $S = 1$ spin with $S_z = +1$ is formed at each site, the up-spin number is unity at each orbital, while the down-spin distribution depends on the orbital. In the AFM state, the configuration of double-occupied orbitals is the same as in the FM

phase, but the single-occupied orbital contains 0.5 up and 0.5 down spins on average, since the $S = 1$ spin direction fluctuates due to the AFM coupling between neighboring $S = 1$ spins. However, as shown in Fig. 1(c), the spin correlation $S(\mathbf{q})$ has a peak at (π, π), indicating the G-AFM structure, where $S(\mathbf{q}) = \sum_{\mathbf{i},\mathbf{j}} e^{i\mathbf{q}\cdot(\mathbf{i}-\mathbf{j})} \langle s_{z\mathbf{i}} s_{z\mathbf{j}} \rangle$ with $s_{z\mathbf{i}} = \sum_{\gamma}(\rho_{\mathbf{i}\gamma\uparrow} - \rho_{\mathbf{i}\gamma\downarrow})/2$. Except for the spin direction, the charge and orbital configuration in the FM/OO phase is the same as in the G-AFM/OO state. As shown in Fig. 1(d), a clear ordering pattern including xy, yz, and zx orbitals is suggested for these FM and AFM phases [13]. Deduced from the present 2×2 result, the proposed bulk orbital ordering in ruthenates is shown in Fig. 1(e). Note that in this pattern xy orbitals occupy only half the Ru sites, while zx (yz) orbitals connect second nearest-neighbor xy orbitals along the x (y) axis. This structure, quite different from a uniform population of the xy orbitals, is natural from the viewpoint of the kinetic energy gain of t_{2g} electrons, with all orbitals contributing to such gain.

Although the results discussed above are exact, they have been obtained using a small-size cluster. Unfortunately, larger clusters cannot be studied due to severe limitations of memory and CPU time. However, it is possible to consider larger lattices by employing a mean-field approximation. For the insulating ground state with static lattice distortions, the mean-field approximation is expected to provide qualitatively correct results. In the actual calculations, only the diagonal portion of the Coulomb interactions in spin and orbital space are included by carrying out a standard Hartree-Fock decoupling procedure, working with the fixed lattice distortions deduced from the 2×2 results. In Fig. 1(f), the mean-field energies vs U' on the 8×8 cluster are depicted at $E_{ph} = 1.0$. It is remarkable that, with increasing U', the ground state changes from CDW, to G-AFM, and finally to FM, in excellent agreement with the 2×2 results [14]. For intermediate values of U', the G-type AFM phase with the hole arrangement observed in experiments is easily obtained, if the lattice distortion to produce the orbital ordering in Fig. 1(e) is assumed. For large U', on the other hand, the FM phase is stabilized [15]. The mean field generates stable phases and their competition is in qualitative agreement with the small-cluster results for $E_{ph} \neq 0$ and $U' \neq 0$, suggesting that the orbital ordering coupled to lattice distortions is essential to explain the magnetic structure of ruthenates.

Now let us discuss intuitively the origin of the complex OO pattern observed here. Because of the Hund coupling, a local $S = 1$ spin is formed by the four electrons, as shown in Fig. 1(b). Note that each orbital includes at least one spin-majority electron, leading to the cancellation of their distortions due to the relation $Q_{x\mathbf{i}} + Q_{y\mathbf{i}} + Q_{z\mathbf{i}} = 0$. Thus, the OO pattern is determined by the choice of orbital occupancy of the excess spin-minority electron. Note that the energy levels of orbitals occupied and unoccupied by this excess electron are $-2E_{ph}$ and $+E_{ph}$, respectively. The two-dimensional network composed of xy orbitals is occupied in a *bipartite* manner by the excess electrons,

to gain kinetic energy (namely, to avoid the total "freezing" of the xy orbitals). Other excess electrons occupy yz and zx orbitals, with mobility only along one-dimensional (1D) chains, coupled to $Q_{x\mathbf{i}}$ and $Q_{y\mathbf{i}}$ distortions, respectively. These distortions should occur in pairs to cancel the in-plane total distortions, since Q_x (Q_y) denotes the elongation along the x (y) direction. Then, half of the 1D chains of yz and zx orbitals are occupied, to avoid the sites with occupied xy orbitals. The above considerations naturally lead to the orbital pattern in Fig. 1(e).

Another interesting aspect of the phase diagram [Fig. 1(a)] is the appearance of a FM/OD phase adjacent to the G-AFM/OO phase, suggesting a competition between metallic FM and insulating AFM states. Since this two-phase competition is a key concept to understand CMR manganites [7], the present result suggests the possibility of CMR-like effects in ruthenates as well. If a small-radius alkaline-earth ion is substituted for Ca or Sr, CMR-like phenomena may be observed in Ru oxides. Note that a two-phase competition has already been observed experimentally in the bilayer ruthenates [16].

To complete the intuitive analysis, the cases of $E_{ph} = 0$ and $U' = J = 0$ are discussed separately. Let us consider the pure Coulombic model $H_{el} = H_{kin} + H_{el-el}$ using the Lanczos method. In Fig. 2(a), the ground state phase diagram on the $(U' - J, J)$ plane is depicted by comparing the energies of the states classified by the z component of total spin. As discussed in the literature of the multiband Hubbard model [17], the FM phase appears for large
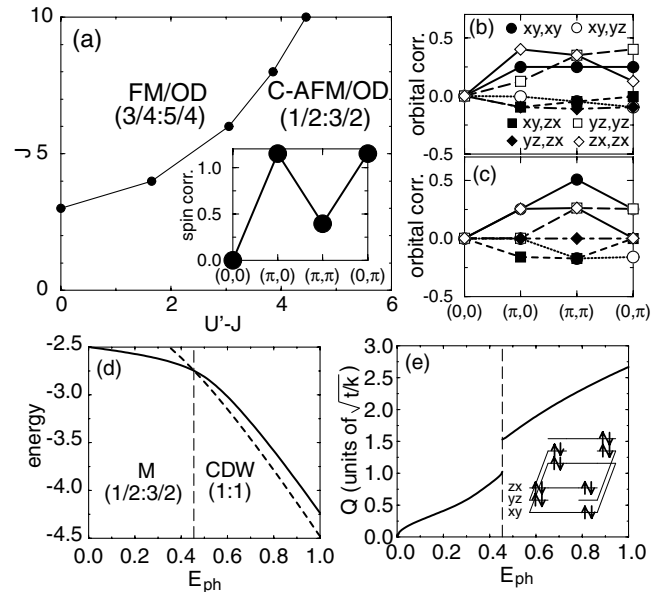

FIG. 2. (a) Ground state phase diagram for the pure Coulombic model H_{el}. Note that only the realistic region $U' - J > 0$ is shown. The inset denotes the spin correlation in the C-AFM phase. (b),(c) Fourier transform of orbital correlation function for FM and C-AFM phases, respectively. (d) Ground state energy vs E_{ph} for the pure phononic model H_{ph}. (e) Average lattice distortion Q vs E_{ph}. In the inset, the electron configuration for the CDW state is shown.

J and small $U' - J$. Although it is difficult to analyze transport properties of the FM phase in this small-cluster calculation, the FM state characterized by 3/4:5/4 is likely metallic, since the orbitals are disordered. In fact, there is no clear peak in the orbital correlation $O_{\gamma\gamma'}(\mathbf{q})$, as shown in Fig. 2(b), where $O_{\gamma\gamma'}(\mathbf{q}) = \sum_{\mathbf{i},\mathbf{j}} e^{i\mathbf{q}\cdot(\mathbf{i}-\mathbf{j})}\langle\rho_{\mathbf{i}\gamma}\rho_{\mathbf{j}\gamma'}\rangle$. For large $U' - J$, the singlet ground state appears, but this is not the Néel state and is instead the C-type AFM state, since the spin correlation function $S(\mathbf{q})$ has two peaks at $\mathbf{q} = (\pi, 0)$ and $(0, \pi)$, not at (π, π), as shown in the inset of Fig. 2(a). Note here that this singlet ground state is doubly degenerate, since there occurs two types of C-AFM states characterized by the peaks of $S(\mathbf{q})$ at $\mathbf{q} = (0, \pi)$ and $(0, \pi)$. This degeneracy originates from the geometry of the two types of possible 1D bands composed of yz and zx orbitals. Considering one of the FM bonds among the $S = 1$ spins of the C-AFM state, the excess electron in the yz (zx) orbital can move along the y (x) direction, providing a kinetic energy gain, while a superexchange interaction occurs in the AFM bonds. Thus, the coexistence of FM and AFM bonds in the C-AFM phase is due to the balance of kinetic energy and superexchange interaction. Since the orbital correlation function in Fig. 2(c) is composed of several orbital patterns of degenerate states, the C-AFM phase is also OD. In short, in the 2×2-plaquette calculation, the singlet ground state of a pure H_{el} is C-AFM and OD if lattice distortions are not included, in disagreement with experiments [5]. The G-AFM state is not stable in a purely Coulombic model due to a Hund coupling energy penalization for its mobile electrons, compared with the C-AFM state that has better electronic mobility.

Consider now the pure phononic model $H_{\text{ph}} = H_{\text{kin}} + H_{\text{el-ph}}$ analyzed by using the relaxation technique. In Figs. 2(d) and 2(e), the ground state energy and the average distortion Q are shown as a function of E_{ph} ($Q = \sum_{\mathbf{i}} \sqrt{Q_{2\mathbf{i}}^2 + Q_{3\mathbf{i}}^2}/4$). For small E_{ph}, the ground state with small Q is characterized by 1/2:3/2. When E_{ph} is further increased, Q abruptly becomes larger and the hole configuration changes to 1:1. In this state, to gain lattice energy, two of the three t_{2g} orbitals are doubly occupied, leading to the orbital-dependent CDW state [see the inset of Fig. 2(e)]. Note that the ground state of H_{ph} is always nonmagnetic without the electron correlation that forbids double occupancy. Then, the existence of a finite Hund coupling, and concomitant Hubbard repulsion, is crucial to reproduce experimental results, as long as it is supplemented by a lattice distortion.

In summary, to understand the magnetic properties of ruthenates, a model with Coulombic and phononic interactions has been analyzed by numerical techniques and mean-field approximations. It has been found that the stabilization of the nontrivial orbital ordering state described here is crucial to understand the 1/2:3/2 G-type AFM phase observed in experiments. Both phononic and Coulombic interactions play an important role in this stabilization. In addition, (i) a competition between FM/OD and AFM/OO phases suggests the possibility of large magnetoresistance effects in ruthenates, and (ii) a FM/OO phase is predicted to exist for ruthenates with large Coulomb interactions.

[1] Y. Maeno *et al.,* Nature (London) **372**, 532 (1994); Y. Maeno, T. M. Rice, and M. Sigrist, Phys. Today **54**, No. 1, 42 (2001).

[2] T. M. Rice and M. Sigrist, J. Phys. Condens. Matter **7**, L643 (1995).

[3] S. Nakatsuji and Y. Maeno, Phys. Rev. Lett. **84**, 2666 (2000); G. Cao *et al.,* Phys. Rev. B **56**, R2916 (1997).

[4] M. Braden *et al.,* Phys. Rev. B **58**, 847 (1998).

[5] T. Mizokawa *et al.,* Phys. Rev. Lett. **87**, 077202 (2001).

[6] S. Nakatsuji and Y. Maeno, Phys. Rev. B **62**, 6458 (2000).

[7] E. Dagotto, T. Hotta, and A. Moreo, Phys. Rep. **344**, 1 (2001).

[8] M. D. Struge, Solid State Phys. **20**, 91 (1967).

[9] It is expected that the key properties of the competing states can be captured even when using a small cluster, since fluctuations are suppressed in the insulating ground state with robust static lattice distortions. This has been extensively documented in manganite studies (see Ref. [7]). However, care is needed to study the metallic phase.

[10] E. Dagotto, Rev. Mod. Phys. **66**, 763 (1994).

[11] In actual calculations, at each step for the relaxation, the electronic portion of the Hamiltonian is exactly diagonalized for a fixed distortion. Iterations are repeated until the system converges to the global ground state.

[12] Phase boundaries are determined by the energy comparison of competing states. Note that the relation $J = 3U'/4$ is just for convenience to depict Fig. 1(a). Other choices of J lead to a similar phase diagram.

[13] A ferro "0:2" xy orbital ordered state was suggested by V. I. Anisimov *et al.* in cond-mat/0011460, but it is different from experiments in Ref. [5]. In our calculations this state is an excited state for $E_{\text{ph}} \lesssim 2.0$. Note that Mizokawa *et al.* (Ref. [5]) assumed a combination of "complex" orbitals, yz and $(xy + izx)/\sqrt{2}$, to explain both the hole distribution and the orbital angular momentum. Since the spin-orbit coupling is not included in our model, the orbital angular momentum is quenched. However, if the spin-orbit interaction among t_{2g} orbitals [K. K. Ng and M. Sigrist, Europhys. Lett. **49**, 473 (2000)] is considered, such complex orbitals could be naturally reproduced. This issue will be studied in future investigations.

[14] Note the factor 2 discrepancy in the energy units between the 2×2 plaquette and 8×8 lattice due to the different boundary conditions.

[15] This phase has not yet been observed experimentally, and it may correspond to a FM insulator.

[16] G. Cao *et al.,* Phys. Rev. B **56**, 5387 (1997).

[17] M. Imada *et al.,* Rev. Mod. Phys. **70**, 1039 (1998).